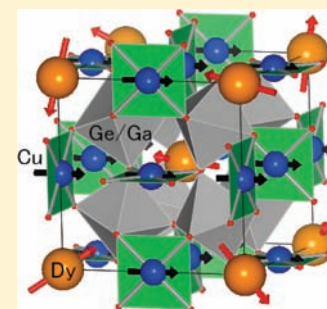


Magnetic Interactions in A-Site-Ordered Perovskites $\text{LnCu}_3(\text{Ge}_{3/4}\text{Ga}_{1/4})_4\text{O}_{12}$ (Ln = La, Dy)

Takashi Saito,^{*,†} Ryuta Yamada,[†] and Yuichi Shimakawa^{†,‡}[†]Institute for Chemical Research, Kyoto University, Gokasho, Uji, Kyoto, 611-0011 Japan[‡]CREST, Japan Science and Technology Agency, Gobancho, Chiyoda-ku, Tokyo, 102-0076 Japan

ABSTRACT: A-site-ordered perovskites $\text{LaCu}_3(\text{Ge}_{3/4}\text{Ga}_{1/4})_4\text{O}_{12}$ and $\text{DyCu}_3(\text{Ge}_{3/4}\text{Ga}_{1/4})_4\text{O}_{12}$ were synthesized, and their magnetism was investigated. Ferromagnetic ordering of the square-planar-coordinated Cu^{2+} spins was observed at 12–13 K in both compounds, and the Dy^{3+} moment in $\text{DyCu}_3(\text{Ge}_{3/4}\text{Ga}_{1/4})_4\text{O}_{12}$ stayed paramagnetic below T_C . The decoupling of the magnetic behavior of Cu^{2+} and Dy^{3+} sublattices revealed the weak magnetic interaction between Cu^{2+} and Dy^{3+} .



INTRODUCTION

The A-site-ordered perovskites $\text{AA}'_3\text{B}_4\text{O}_{12}$ (Figure 1) are attracting much interest due to their large variety of physical

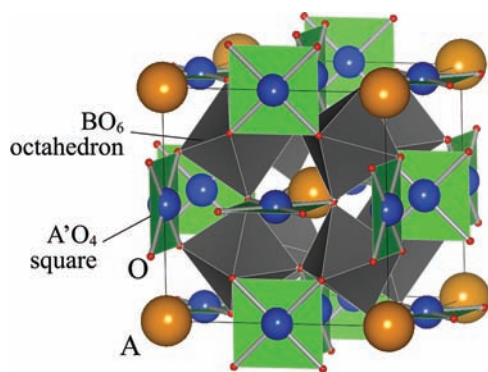


Figure 1. Crystal structure of A-site-ordered perovskites $\text{AA}'_3\text{B}_4\text{O}_{12}$.

properties.^{1,2} Because they contain transition-metal ions at both A' and B sites, one sees not only the B–B interaction seen in many ABO_3 perovskite oxides but also A'–A' and A'–B interactions.^{3–8} When the A' and B-site ions respectively are magnetic and nonmagnetic species, we can see unique magnetic interactions in the A'-site sublattice. In $\text{CaCu}_3\text{Sn}_4\text{O}_{12}$ and $\text{CaCu}_3\text{Ge}_4\text{O}_{12}$, for example, only Cu^{2+} spins ($S = 1/2$) at the A' site contribute to the magnetic properties, and the interaction is ferromagnetic.⁹ The A'-site ferromagnetism originates from the direct exchange interaction between the spins at the square-planar-coordinated Cu site that are perpendicular to each other. In $\text{CaCu}_3\text{Ti}_4\text{O}_{12}$, on the other hand, the A'-site Cu^{2+} spins align antiferromagnetically because of the superexchange interaction via $\text{Cu}-\text{O}-\text{Ti}-\text{O}-\text{Cu}$.^{10–12} The antiferromagnetic interaction is mediated by the hybridization of the Ti-3d orbital with the Cu-3d and O-2p orbitals.^{9,13,14} Thus, in the $\text{CaCu}_3\text{B}_4\text{O}_{12}$

system with the nonmagnetic B-site ions, either ferromagnetism or antiferromagnetism arises within the cubic A'-site $S = 1/2$ spin sublattice.¹⁵

Because most of the A-site-ordered perovskites $\text{AA}'_3\text{B}_4\text{O}_{12}$ have cubic crystal structures, they provide interesting systems for studying magnetic interactions of spins on the cubic A, A', and B sublattices. The magnetic interaction between the A and A' ions in A-site-ordered perovskite oxides was investigated recently. In $\text{Ln}_{2/3}\text{Cu}_3\text{Ti}_4\text{O}_{12}$ (Ln = lanthanides), antiferromagnetic transition of the A'-site Cu^{2+} spins ($S = 1/2$) was observed and the magnetic moments of the A-site Ln^{3+} ions showed paramagnetic behaviors down to the lowest temperature measured.¹⁶ The antiferromagnetic transition temperature decreased slightly when the lattice dimension was increased by using larger A-site Ln^{3+} ions.¹⁷ Thus, the results evidently show that the magnetic interaction between the A-site ions and the antiferromagnetically ordered A'-site ions is very weak and that the spins of the A- and A'-site sublattices are decoupled. In antiferromagnetic $\text{Ln}_{2/3}\text{Cu}_3\text{Ti}_4\text{O}_{12}$ with a $[1\ 1\ 1]$ propagation vector, the A site is surrounded by the six nearest up-spin Cu^{2+} ions and the 12 next-nearest down-spin Cu^{2+} ions, and the net internal magnetic field at the A site can be canceled out.

It is of particular interest what happens to the magnetic behavior of the A-site Ln moments in the ferromagnetically ordered A'-site sublattice spin system. In this study, attempts were made to introduce a magnetic Ln^{3+} ion to the A site in ferromagnetic $\text{CaCu}_3\text{Ge}_4\text{O}_{12}$. Dy^{3+} was chosen to substitute for Ca^{2+} because of its largest magnetic moment in the Ln^{3+} series, and we succeeded in synthesizing $\text{DyCu}_3(\text{Ge}_{3/4}\text{Ga}_{1/4})_4\text{O}_{12}$, in which both A-site Dy^{3+} and A'-site Cu^{2+} have magnetic moments. $\text{LaCu}_3(\text{Ge}_{3/4}\text{Ga}_{1/4})_4\text{O}_{12}$, with a magnetic moment only at the Cu^{2+} site, was also synthesized as a reference

Received: November 30, 2011

Published: April 19, 2012

compound for the magnetic study. The magnetic behaviors and the interactions of the A-site Dy^{3+} and A'-site Cu^{2+} are discussed here.

EXPERIMENTAL SECTION

A high-pressure technique was used for the sample preparation, because high-pressure and high-temperature conditions are required for the syntheses of many of the A-site-ordered perovskites. Stoichiometric mixtures of raw materials (Dy_2O_3 , CuO , GeO_2 , Ga_2O_3 , and La_2O_3) were sealed in Pt capsules and were heated at $1200\text{ }^\circ\text{C}$ for 30 min under a pressure of 9 GPa produced by using a cubic-anvil press. Then the materials were quenched to room temperature and the pressure was subsequently released. The Dy_2O_3 and La_2O_3 had been preheated at $1000\text{ }^\circ\text{C}$ in air to eliminate carbonate impurities.

Synchrotron X-ray diffraction (SXRD) patterns of the polycrystalline samples were collected using a Debye–Scherrer camera installed at BL02B2 of SPring-8, Japan. The wavelength was 0.77514 \AA , and the diffraction patterns were recorded on imaging plates. Rietveld refinement of the crystal structure was done using the RIETAN2000 program. Magnetic susceptibility in an external field of 0.01 T and isothermal magnetizations at 5 K were measured by using a SQUID magnetometer (Magnetic Property Measurement System, Quantum Design).

RESULTS AND DISCUSSION

We first tried to synthesize $\text{Dy}_{2/3}\text{Cu}_3\text{Ge}_4\text{O}_{12}$, which was expected to have 1/3 A-site deficiency to keep the charge neutrality of the sample, as in the case of $\text{Ln}_{2/3}\text{Cu}_3\text{Ti}_4\text{O}_{12}$.¹⁷ Thus the obtained sample contained a large amount of unreacted GeO_2 together with an A-site-ordered perovskite phase whose composition therefore seemed to be $\text{DyCu}_3(\text{Cu,Ge})_4\text{O}_{12}$. This may be partly because $\text{Dy}_{2/3}\text{Cu}_3\text{Ge}_4\text{O}_{12}$, with 1/3 A-site deficiency, is expected to have much lower density than $\text{DyCu}_3(\text{Cu,Ge})_4\text{O}_{12}$ and should therefore become energetically unfavorable compared to $\text{DyCu}_3(\text{Cu,Ge})_4\text{O}_{12}$ under high pressures. Nonmagnetic Ga^{3+} was then introduced instead of Cu^{2+} at 1/4 of the B site, yielding $\text{DyCu}_3(\text{Ge}_{3/4}\text{Ga}_{1/4})_4\text{O}_{12}$. It is important to note here that both Ga^{3+} and Ge^{4+} have the same $3d^{10}$ configurations. Here $\text{DyCu}_3(\text{Ge}_{3/4}\text{Ga}_{1/4})_4\text{O}_{12}$ has full occupancy at the A site with a perovskite-type close-packed structure and is therefore expected to be stabilized under high pressures. $\text{LaCu}_3(\text{Ge}_{3/4}\text{Ga}_{1/4})_4\text{O}_{12}$ was also obtained, with an A-site-ordered perovskite structure.

Figure 2 shows the SXRD patterns of $\text{LnCu}_3(\text{Ge}_{3/4}\text{Ga}_{1/4})_4\text{O}_{12}$ ($\text{Ln} = \text{La, Dy}$), and the results of the refinements are listed in Tables 1 and 2. Each diffraction pattern was well indexed with a cubic unit cell with the space group $Im\bar{3}$ and was reproduced with an A-site-ordered perovskite model. The absence of any superstructure reflections or forbidden reflections of the $Im\bar{3}$ unit cell indicates the random distribution of $\text{Ge}^{4+}/\text{Ga}^{3+}$ at the B site. We note here that although by X-ray diffraction it is difficult to distinguish between isoelectronic Ge^{4+} and Ga^{3+} because their atomic scattering factors are similar, there should be a detectable difference in the bond distances to their neighboring oxygen if they order at the B site, because they have different ionic radii (0.53 \AA for Ge^{4+} and 0.62 \AA for Ga^{3+} with octahedral coordination by oxygen¹⁸). The crystal structures of the two compounds are quite similar to each other. The bond valence sum (BVS) values, which are the ionic valences empirically estimated from the bond distances between cations and coordinated anions, suggest that the A'-site Cu is divalent,

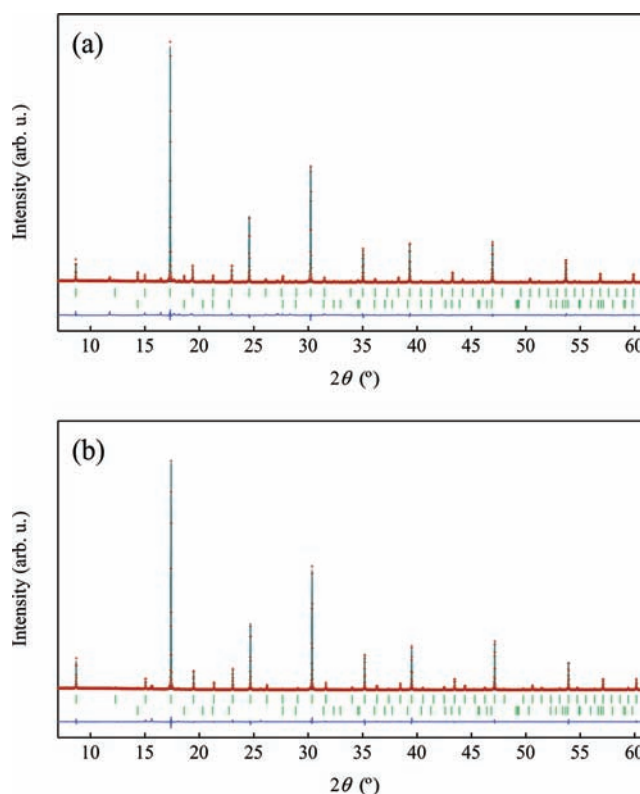


Figure 2. SXRD data and the Rietveld refinement profiles of $\text{LaCu}_3(\text{Ge}_{3/4}\text{Ga}_{1/4})_4\text{O}_{12}$ (a) and $\text{DyCu}_3(\text{Ge}_{3/4}\text{Ga}_{1/4})_4\text{O}_{12}$ (b). The observed data are shown as (+) marks, and the calculated profiles are shown as solid lines (—). The differences between the observed and the calculated intensities are shown at the bottom. Tick marks (|) represent the positions of the allowed diffraction peaks of $\text{LnCu}_3(\text{Ge}_{3/4}\text{Ga}_{1/4})_4\text{O}_{12}$ (upper row) and GeO_2 impurity (bottom row).

Table 1. Results of the Rietveld Refinement of $\text{LnCu}_3(\text{Ge}_{3/4}\text{Ga}_{1/4})_4\text{O}_{12}$ ($\text{Ln} = \text{La, Dy}$)^{a,b}

	Ln	La	Dy
a (Å)		7.28611(1)	7.25586(1)
V (Å ³)		386.800(1)	382.0036(7)
U_{iso} (Å ²)		0.0030(1)	0.0006(1)
O	x	0.2995(4)	0.2984(3)
	y	0.1820(5)	0.1792(4)
R_{wp} (%)		4.36	3.70
R_p (%)		2.62	2.02

^aCubic space group $Im\bar{3}$ (No. 204) was adopted for both refinements, where the atomic positions were Ln $2a$ (0, 0, 0)(A site), Cu $6b$ (0, 1/2, 1/2)(A' site), Ge/Ga $8c$ (1/4, 1/4, 1/4)(B site), and O $24g$ ($x, y, 0$).

^bThe Ge/Ga ratio was fixed to 3 in the refinement.

giving a charge state of $\text{Ln}^{3+}\text{Cu}^{2+}_3(\text{Ge}^{4+}_{3/4}\text{Ga}^{3+}_{1/4})_4\text{O}^{2-}_{12}$ ($\text{Ln} = \text{La, Dy}$). Here $\text{DyCu}_3(\text{Ge}_{3/4}\text{Ga}_{1/4})_4\text{O}_{12}$ contains magnetic Dy^{3+} and Cu^{2+} ions respectively at the A and A' sites and nonmagnetic Ge^{4+} and Ga^{3+} at the B site. On the other hand, A'-site Cu^{2+} is the only magnetic ion for $\text{LaCu}_3(\text{Ge}_{3/4}\text{Ga}_{1/4})_4\text{O}_{12}$.

The temperature dependence of the magnetic susceptibility and the inverse susceptibility for $\text{LaCu}_3(\text{Ge}_{3/4}\text{Ga}_{1/4})_4\text{O}_{12}$ are shown in Figure 3a and its inset, where one clearly sees a ferromagnetic transition with a Curie temperature $T_C = 12\text{ K}$. An effective magnetic moment $p_{\text{eff}} = 1.781(6)\mu_B/\text{Cu}$ and Weiss

Table 2. Selected Bond Lengths, Bond Angles, and Bond Valence Sums (BVS) for the Refined Structures of $\text{LnCu}_3(\text{Ge}_{3/4}\text{Ga}_{1/4})_4\text{O}_{12}$ (Ln = La, Dy)

	Ln	La	Dy
$d(\text{Ln}-\text{O})$ (Å) [$\times 12$]		2.554(3)	2.526(3)
$d(\text{Cu}-\text{O})$ (Å) [$\times 4$]		1.973(3)	1.957(2)
$d(\text{Cu}-\text{O})$ (Å) [$\times 4$]		2.739(3)	2.749(3)
$d(\text{Cu}-\text{O})$ (Å) [$\times 4$]		3.183(3)	3.179(2)
$d(\text{Ge}/\text{Ga}-\text{O})$ (Å) [$\times 6$]		1.922(1)	1.9178(8)
Cu–O–Cu (deg)		100.0 (1)	99.49(9)
B–O–B (deg)		142.8(2)	142.1(1)
Cu–O–B (deg)		108.19 (9)	108.36(7)
BVS(Cu)		1.97	2.04

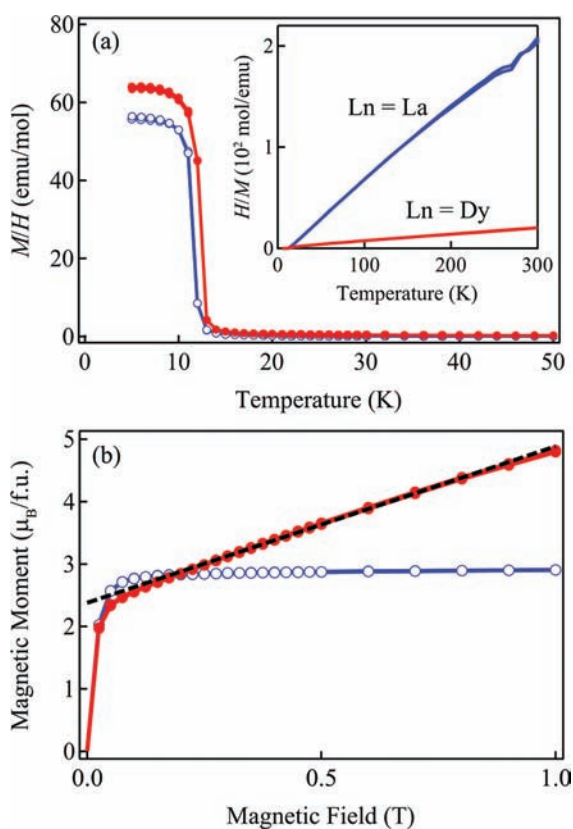


Figure 3. Magnetic susceptibility at 0.01 T (a) and isothermal magnetization at 5 K (b) of $\text{LaCu}_3(\text{Ge}_{3/4}\text{Ga}_{1/4})_4\text{O}_{12}$ (○) and $\text{DyCu}_3(\text{Ge}_{3/4}\text{Ga}_{1/4})_4\text{O}_{12}$ (●). The inverse magnetic susceptibilities are shown in the inset of (a), and the extrapolation of the magnetization data above 0.15 to 0 T for $\text{DyCu}_3(\text{Ge}_{3/4}\text{Ga}_{1/4})_4\text{O}_{12}$ is shown in (b) as a dashed line.

temperature $\theta_{\text{CW}} = 14.4(2)$ K were obtained from Curie–Weiss fitting between 100 and 300 K, indicating ferromagnetic ordering of the A'-site Cu^{2+} spins with $S = 1/2$. The isothermal magnetization of $\text{LaCu}_3(\text{Ge}_{3/4}\text{Ga}_{1/4})_4\text{O}_{12}$ at 5 K, shown in Figure 3b, confirmed a ferromagnetic behavior with a saturation moment of $M_S \approx 2.9 \mu_B$ per formula unit, consistently. The ferromagnetism of $\text{LaCu}_3(\text{Ge}_{3/4}\text{Ga}_{1/4})_4\text{O}_{12}$ resembles that of $\text{CaCu}_3\text{Ge}_4\text{O}_{12}$: $T_C = 13$ K, $p_{\text{eff}} = 1.76 \mu_B/\text{Cu}$, $\theta_{\text{CW}} = 16.4$ K, and $M_S \approx 2.7 \mu_B$ per formula unit.⁹ We can thus conclude that the observed ferromagnetic behavior of $\text{LaCu}_3(\text{Ge}_{3/4}\text{Ga}_{1/4})_4\text{O}_{12}$ originates from the A'-site Cu^{2+} spins and that the partial substitution of Ga^{3+} for Ge^{4+} at the B site does not cause any difference in the ferromagnetism. The ferromagnetism of

$\text{LaCu}_3(\text{Ge}_{3/4}\text{Ga}_{1/4})_4\text{O}_{12}$ should, like that of $\text{CaCu}_3\text{Ge}_4\text{O}_{12}$, be attributed to the Cu–Cu direct-exchange interaction.^{9,15}

A similar ferromagnetic transition, with $T_C = 13$ K, was also seen in the magnetic susceptibility of $\text{DyCu}_3(\text{Ge}_{3/4}\text{Ga}_{1/4})_4\text{O}_{12}$, as shown in Figure 3a. The inverse susceptibility (shown in the inset) has a linear temperature dependence well above T_C , and Curie–Weiss fitting of the susceptibility between 100 and 300 K gave a Curie constant $C = 13.2(1)$ emu/K·mol per formula unit and $\theta_{\text{CW}} = -5.1(5)$ K. Assuming $p_{\text{eff}}^2 = p_{\text{eff}}(\text{Dy}^{3+})^2 + 3p_{\text{eff}}(\text{Cu}^{2+})^2$ with total angular momentum $J = 15/2$ for Dy^{3+} and spin $S = 1/2$ for Cu^{2+} , one can expect $p_{\text{eff}} = 11.06$, which corresponds to $C = 15.3$ emu/K·mol per formula unit. This is quite close to the value obtained from the experiment. The small and negative value of θ_{CW} indicates the existence of a weak antiferromagnetic interaction between the large Dy^{3+} moments, because the large Dy^{3+} moment dominates the paramagnetic moment ($p_{\text{eff}}(\text{Dy}^{3+})^2 \gg 3p_{\text{eff}}(\text{Cu}^{2+})^2$) above T_C . The isothermal magnetization of $\text{DyCu}_3(\text{Ge}_{3/4}\text{Ga}_{1/4})_4\text{O}_{12}$ at 5 K shown in Figure 3b is also consistent with such a behavior. Extrapolation of the magnetization above 0.15 to 0 T gives a value of $M_0 = 2.38(1) \mu_B$ per formula unit, indicating ferromagnetic alignment of Cu^{2+} spins with $S = 1/2$. The linear increase in magnetic moment with increasing magnetic field is indicative of the paramagnetic nature of the Dy^{3+} moments. Thus, in $\text{DyCu}_3(\text{Ge}_{3/4}\text{Ga}_{1/4})_4\text{O}_{12}$ only Cu^{2+} spins at the A' site ordered ferromagnetically, while the Dy^{3+} moments at the A site remained paramagnetic down to the lowest temperature we measured (5 K). The similarity of the transition temperatures between $\text{LaCu}_3(\text{Ge}_{3/4}\text{Ga}_{1/4})_4\text{O}_{12}$ and $\text{DyCu}_3(\text{Ge}_{3/4}\text{Ga}_{1/4})_4\text{O}_{12}$ indicates the decoupling of the A-site Dy^{3+} and A'-site Cu^{2+} sublattices. The slight difference in the T_C can be explained by the difference in the Cu–Cu bond distance. The main magnetic interaction in these compounds is the Cu–Cu direct-exchange interaction, and the Cu–Cu bond distance, which is equal to half of the lattice parameter, determines the magnetic transition temperature. It is thus reasonable for $\text{DyCu}_3(\text{Ge}_{3/4}\text{Ga}_{1/4})_4\text{O}_{12}$, with a shorter lattice parameter, to have a higher T_C than $\text{LaCu}_3(\text{Ge}_{3/4}\text{Ga}_{1/4})_4\text{O}_{12}$.

Note that the A-site spin sublattice decouples with either antiferromagnetic or ferromagnetic A'- Cu^{2+} spin sublattice. In an antiferromagnetic A'-site spin sublattice such as in $\text{Ln}_{2/3}\text{Cu}_3\text{Ti}_4\text{O}_{12}$, the A site is surrounded by the six nearest up-spin Cu^{2+} ions and the 12 down-spin Cu^{2+} ions, and the net internal magnetic field at the A site can be canceled out. In the present $\text{DyCu}_3(\text{Ge}_{3/4}\text{Ga}_{1/4})_4\text{O}_{12}$, in contrast, the A site is surrounded by the nearest and second-nearest ferromagnetically ordered Cu^{2+} spins below T_C , and those neighboring spins produce an internal magnetic field at the A site. Even in the ferromagnetic internal field, the A-site Ln^{3+} moment sublattice decouples with the A'-site Cu spin sublattice. It is also interesting to note here that the ferromagnetically ordered A'-site Cu^{2+} spin sublattice strongly couples with the B-site magnetic sublattice. In $\text{CaCu}_3\text{Mn}_4\text{O}_{12}$, for instance, spins of both the A'-site Cu^{2+} and B-site Mn^{4+} sublattices align ferromagnetically, and the A'-site and B-site spin sublattices couple antiferromagnetically, leading to the ferrimagnetism with the transition temperature over room temperature.¹⁹ This is in sharp contrast to the present system, where the magnetic moments of Ln^{3+} at the A site behave independently of the A'-site Cu^{2+} spin sublattice. Because of the very low lying 4f levels in the Ln^{3+} ions, the magnetic interactions between the A and A' sublattices are very weak for both the ferromagnetic and antiferromagnetic A'-site Cu^{2+} spin sublattice systems.

CONCLUSIONS

Novel A-site-ordered perovskites $\text{LnCu}_3(\text{Ge}_{3/4}\text{Ga}_{1/4})_4\text{O}_{12}$ (Ln = La, Dy) were synthesized under high-pressure and high-temperature conditions. They both crystallize in the cubic $Im\bar{3}$ space group, where magnetic Cu^{2+} is located at the A' site and nonmagnetic Ge^{4+} and Ga^{3+} are randomly distributed at the B site. $\text{DyCu}_3(\text{Ge}_{3/4}\text{Ga}_{1/4})_4\text{O}_{12}$ provides a unique system to investigate the magnetic interaction between the A-site and A'-site spin sublattices because the B-site ($\text{Ge}_{3/4}\text{Ga}_{1/4}$) is nonmagnetic. Both $\text{DyCu}_3(\text{Ge}_{3/4}\text{Ga}_{1/4})_4\text{O}_{12}$ and $\text{LaCu}_3(\text{Ge}_{3/4}\text{Ga}_{1/4})_4\text{O}_{12}$ show ferromagnetic ordering of Cu^{2+} spins ($S = 1/2$) at 12–13 K because of the Cu–Cu direct exchange interaction. The Dy^{3+} moment in $\text{DyCu}_3(\text{Ge}_{3/4}\text{Ga}_{1/4})_4\text{O}_{12}$ stays paramagnetic down to 5 K even with the internal magnetic field produced by the ferromagnetically aligned A'-site Cu^{2+} spins, demonstrating a very weak magnetic coupling between A'-site Cu^{2+} and A-site Dy^{3+} . The result also shows a sharp contrast to the strong antiferromagnetic coupling between the A'- and B-site spin sublattices.

AUTHOR INFORMATION

Corresponding Author

*E-mail: saito@scl.kyoto-u.ac.jp.

Notes

The authors declare no competing financial interest.

ACKNOWLEDGMENTS

The synchrotron radiation experiments were performed at SPring-8 with the approval of the Japan Synchrotron Radiation Research Institute. This work was partly supported by the Global COE Program (No. B09), Grants-in-Aid for Scientific Research (Nos. 22740227 and 19GS0207), the Joint Project of Chemical Synthesis Core Research Institutions from MEXT of Japan, and the CREST program of the Japan Science and Technology Agency.

REFERENCES

- (1) Vasil'ev, A. N.; Volkova, O. S. *Low Temp. Phys.* **2007**, *33*, 895.
- (2) Shimakawa, Y. *Inorg. Chem.* **2008**, *47*, 8562.
- (3) Zeng, Z.; Greenblatt, M.; Subramanian, M. A.; Croft, M. *Phys. Rev. Lett.* **1999**, *82*, 3164.
- (4) Subramanian, M. A.; Li, D.; Duan, N.; Reisner, B. A.; Sleight, A. W. *J. Solid State Chem.* **2000**, *151*, 323.
- (5) Kobayashi, W.; Terasaki, I.; Takeya, J.; Tsukada, I.; Ando, Y. *J. Phys. Soc. Jpn.* **2004**, *73*, 2373.
- (6) Prodi, A.; Gilioli, E.; Gauzzi, A.; Licci, F.; Marezio, M.; Bolzoni, F.; Huang, Q.; Santoro, A.; Lin, J. W. *Nat. Mater.* **2004**, *3*, 48.
- (7) Yamada, I.; Takata, K.; Hayashi, N.; Shinohara, S.; Azuma, M.; Mori, S.; Muranaka, S.; Shimakawa, Y.; Takano, M. *Angew. Chem., Int. Ed.* **2008**, *47*, 7032.
- (8) Long, Y. W.; Hayashi, N.; Saito, T.; Azuma, M.; Muranaka, S.; Shimakawa, Y. *Nature* **2009**, *458*, 60.
- (9) Shiraki, H.; Saito, T.; Yamada, T.; Tsujimoto, M.; Azuma, M.; Kurata, H.; Isoda, S.; Takano, M.; Shimakawa, Y. *Phys. Rev. B* **2007**, *76*, 140403(R).
- (10) Ramirez, A. P.; Subramanian, M. A.; Gardel, M.; Blumberg, G.; Li, D.; Vogt, T.; Shapiro, S. M. *Solid State Commun.* **2000**, *115*, 217.
- (11) Koitzsch, A.; Blumberg, G.; Gozar, A.; Dennis, B.; Ramirez, A. P.; Trebst, S.; Wakimoto, S. *Phys. Rev. B* **2002**, *65*, 052406.
- (12) Kim, Y. J.; Wakimoto, S.; Shapiro, S. P.; Gehring, M.; Ramirez, A. P. *Solid State Commun.* **2002**, *121*, 625.
- (13) He, L.; Neaton, J. B.; Cohen, M. H.; Vanderbilt, D.; Homes, C. *Phys. Rev. B* **2002**, *65*, 214112.
- (14) Mizumaki, M.; Saito, T.; Shiraki, H.; Shimakawa, Y. *Inorg. Chem.* **2009**, *48*, 3499.
- (15) Shimakawa, Y.; Shiraki, H.; Saito, T. *J. Phys. Soc. Jpn.* **2008**, *77*, 113702(L).
- (16) Dittl, A.; Krohns, S.; Sebald, J.; Schrettle, F.; Hemmida, M.; Krug von Nidda, H.-A.; Riegg, S.; Reller, A.; Ebbinghaus, S. G.; Loidl, A. *Eur. Phys. J. B* **2011**, *79*, 391.
- (17) Bochu, B.; Deschizeaux, M. N.; Joubert, J. C.; Collomb, A. J.; Chenavas, J.; Marezio, M. *J. Solid State Chem.* **1979**, *29*, 291.
- (18) Shannon, R. D. *Acta Crystallogr. A* **1976**, *32*, 751.
- (19) Sánchez-Benítez, J.; Alonso, J. A.; Martínez-Lope, M. J.; Casais, M. T.; Martínez, J. L.; de Andrés, A.; Fernández-Díaz, M. T. *Chem. Mater.* **2003**, *15*, 2193.